$A(\vec{e},e'\vec{p})B$ responses: From bare nucleons to complex nuclei

Javier R. Vignote,[1] M. C. Martínez,[2] J. A. Caballero,[2] E. Moya de Guerra,[3] and J. M. Udias[1]
[1]*Departamento de Física Atómica, Molecular y Nuclear Universidad Complutense de Madrid, E-28040 Madrid, Spain*
[2]*Departamento de Física Atómica, Molecular y Nuclear Universidad de Sevilla, Apdo. 1065, E-41080 Sevilla, Spain*
[3]*Instituto de Estructura de la Materia, CSIC, Serrano 123, E-28006 Madrid, Spain*
(Received 17 December 2003; revised manuscript received 8 June 2004; published 18 October 2004)

We study the occurrence of factorization in polarized and unpolarized observables in coincidence quasielastic electron scattering. Starting with the relativistic distorted wave impulse approximation, we reformulate the effective momentum approximation and show that the latter leads to observables which factorize under some specific conditions. Within this framework, the role played by final state interactions and, in particular, by the spin-orbit term is explored. Connection with the nonrelativistic formalism is studied in depth. Numerical results are presented to illustrate the analytical derivations and to quantify the differences between factorized and unfactorized approaches.

DOI: 10.1103/PhysRevC.70.044608 PACS number(s): 25.30.Rw, 24.10.Jv, 21.60.Cs

I. INTRODUCTION

Quasielastic $(e,e'p)$ reactions have provided over the years an enormous wealth of information on nuclear structure, particularly, on single particle degrees of freedom: energies, momentum distributions and spectroscopic factors of nucleons inside nuclei [1–3]. In recent years important efforts have been devoted to provide more realistic theoretical descriptions of these processes [4–16]. However, there are still uncertainties associated to the various ingredients that enter in the reaction dynamics: final state interactions (FSI), off-shell effects, nuclear correlations, relativistic degrees of freedom or meson exchange currents (MEC). These ingredients affect the evaluation of electron scattering observables and hence lead to ambiguities in the information on the nuclear and nucleon structure that can be extracted from experiments. In recent years, electron beam polarization as well as polarization degrees of freedom for the outgoing nucleon can be measured, what makes it possible to extract a new wealth of observables from quasielastic $(\vec{e},e'\vec{p})$ reactions. For instance, ratios of transferred polarizations are used to measure ratios of nucleon form factors.

One of the basic results which has made $(e,e'p)$ reactions so appealing for investigations of single particle properties is the factorized approach [1,17,18]. Within this approximation, the $(e,e'p)$ differential cross section factorizes into a single-nucleon cross section, describing electron proton scattering, and a spectral function which gives the probability to find a proton in the target nucleus with selected values of energy and momentum compatible with the kinematics of the process. The simplicity of the factorized result makes it possible to get a clear image of the physics contained in the problem. Even being known that factorization does not hold in general, it is often assumed that the breakdown of factorization is not too severe, and then it is still commonplace to use factorized calculations for few body systems or for inclusive scattering. The importance of factorization lies on the fact that the interpretation of experimental data is still usually based on this property by defining an effective spectral function that is extracted from experiment in the form of a reduced cross section. Assuming that factorization holds at least approximately, reduced cross section would yield information on momentum distributions of the nucleons inside the nucleus. On the other hand, these momentum distributions would cancel when taking ratios of cross sections and consequently these ratios might give information on the electromagnetic form factors of the nucleons [19,20].

In spite of the importance of the factorization assumption, there have been however almost no formal (and very few quantitative) studies of its validity. So far, it has been shown by different authors [3,18,21] that in the nonrelativistic case and when using plane waves to describe the ejected nucleon [plane wave impulse approximation (PWIA)], factorization holds exactly for the *unpolarized cross section*. When interactions in the final state are included [distorted wave impulse approximation (DWIA)], then certain further assumptions are needed to recover the factorized result [3]. The meaning and importance of the additional assumptions required to attain a factorized result has not been quantitatively studied thoroughly.

In the relativistic case, factorization of the unpolarized cross section is broken even without FSI, due to the negative energy components of the bound nucleon wave function [18,21]. A quantitative estimate of the breakdown of factorization is lacking for the relativistic case when taking into account FSI.

Furthermore, there has not been any study of the validity of the factorization picture for polarization observables, even though this factorized picture is implicitly assumed when using ratios of transferred polarizations to determine nucleon form factors [19,20].

Within a nonrelativistic framework, the breakdown of factorization has been usually interpreted as due to the spin-orbit dependent optical potentials. We note however, that other effects such as the Coulomb distortion of the electron waves, and contributions beyond the impulse approximation (IA) such as MEC, play also a role in breaking factorization. In the particular case of the plane wave limit (i.e., neglecting FSI between the ejected proton and the residual nucleus) factorization is strictly satisfied in IA at the level of the tran-

sition amplitude [3,18]. This contrasts strongly with the relativistic formalism, where the enhancement of the lower components of the bound nucleon wave function destroys factorization of the transition amplitude even in the case of no FSI. Hence, an important difference between relativistic and nonrelativistic approaches already emerges in the plane wave limit. Whereas factorization holds in nonrelativistic PWIA, it does not in the relativistic plane wave impulse approximation (RPWIA), which includes negative-energy components in the bound nucleon wave function [18,21].

As mentioned above, the mechanism that breaks factorization has been only established for the unpolarized cross section in the nonrelativistic approach. Here we explore such mechanisms for both polarized and unpolarized observables starting from the more complex relativistic distorted wave impulse approximation (RDWIA) and making simplifying assumptions that lead to factorization. We make also the connection with the nonrelativistic framework and present conclusions that are valid in both relativistic and nonrelativistic cases. It is important to point out that most of the $(e,e'p)$ experiments performed recently involved energies and momenta high enough to make compulsory the use of relativistic nucleon dynamics. Within this context, the RDWIA, which incorporates kinematical and dynamical relativistic effects, has proved its capability to explain polarized and unpolarized $(e,e'p)$ experimental data [6,9–11]. Starting from the RDWIA, the effective momentum approximation (EMA-noSV), originally introduced by Kelly [22], is reformulated here paying special attention to aspects concerned with the property of factorization. In addition, an analysis is made of the various assumptions that lead to factorized polarized and unpolarized observables and which are mainly linked to the spin-orbit dependence of the problem. Finally, a quantitative estimate of the validity (or breakdown) of factorization is made for different observables that are commonly extracted from $(e,e'p)$ experiments.

The paper is organized as follows: in Sec. II we outline the basic RDWIA formalism and revisit the EMA-noSV approach, emphasizing its connection with the factorized approximation. In Sec. III we present our analysis for polarized and unpolarized observables, deriving the specific conditions which lead to *factorization*. In Sec. IV we concentrate on reduced cross sections and connect them to the momentum distributions. Results for polarized and unpolarized observables are presented in Sec. V. Numerical calculations performed within different approaches are compared. Finally, in Sec. VI we draw our conclusions.

II. RELATIVISTIC DISTORTED WAVE IMPULSE APPROXIMATION (RDWIA)

The RDWIA has been described in detail in previous works (see for instance [6,11]). In this section we limit our attention to those aspects needed for later discussion of the results presented. In RDWIA the one body nucleon current

$$J^{\mu}(\omega,\boldsymbol{q}) = \int d\boldsymbol{p}\,\overline{\psi}_F^{S_F}(\boldsymbol{p}+\boldsymbol{q})\hat{J}^{\mu}\psi_{\kappa_b}^{\mu_b}(\boldsymbol{p}), \tag{1}$$

where ω and $\boldsymbol{q}$ are the energy and momentum of the exchanged virtual photon, is calculated with relativistic $\psi_{\kappa_b}^{\mu_b}$ and $\psi_F^{S_F}$ wave functions for initial bound and final outgoing nucleons, respectively, and with relativistic nucleon current operator $\hat{J}^{\mu}$.

The bound state wave function is a four-spinor with well defined angular momentum quantum numbers κ_b, μ_b corresponding to the shell under consideration. In momentum space it is given by

$$\psi_{\kappa_b}^{\mu_b}(\boldsymbol{p}) = \frac{1}{(2\pi)^{3/2}}\int d\boldsymbol{r}e^{-i\boldsymbol{p}\cdot\boldsymbol{r}}\psi_{\kappa_b}^{\mu_b}(\boldsymbol{r}) = (-i)^{\ell_b}\begin{pmatrix} g_{\kappa_b}(p) \\ S_{\kappa_b}f_{\kappa_b}(p)\dfrac{\boldsymbol{\sigma}\cdot\boldsymbol{p}}{p}\end{pmatrix}\Phi_{\kappa_b}^{\mu_b}(\hat{\boldsymbol{p}}), \tag{2}$$

which is the eigenstate of total angular momentum $j_b=|\kappa_b|-1/2$, and $\Phi_{\kappa_b}^{\mu_b}(\hat{\boldsymbol{p}})$ are the spinor harmonics

$$\Phi_{\kappa_b}^{\mu_b}(\hat{\boldsymbol{p}}) = \sum_{m_{\ell_b}h}\left\langle \ell_b m_{\ell_b}\frac{1}{2}h|j_b\mu_b\right\rangle Y_{\ell_b}^{\mu_b}(\hat{\boldsymbol{p}})\chi_{1/2}^{h}, \tag{3}$$

with $\ell_b=\kappa_b$ if $\kappa_b>0$ and $\ell_b=-\kappa_b-1$ if $\kappa_b<0$.

The wave function for the outgoing proton is a solution of the Dirac equation containing scalar (S) and vector (V) optical potentials [6,7]. For a nucleon scattered with asymptotic momentum $\boldsymbol{p}_F$ and spin projection s_F, its expression is

$$\psi_F^{S_F}(\boldsymbol{p}) = 4\pi\sqrt{\frac{E_F+M}{2E_F}}\sum_{\kappa\mu m}e^{-i\delta_{\kappa}^{*}}i^{\ell} \times\left\langle \ell m\frac{1}{2}s_F|j\mu\right\rangle Y_{\ell}^{m*}(\hat{\boldsymbol{p}}_F)\psi_{\kappa}^{\mu}(\boldsymbol{p}). \tag{4}$$

As the optical potential may be in general complex the phase shifts and radial functions are also complex, and the wave function $\psi_{\kappa}^{\mu}(\boldsymbol{p})$ is given by

$$\psi_{\kappa}^{\mu}(\boldsymbol{p}) = (-i)^{\ell}\begin{pmatrix} g_{\kappa}^{*}(p) \\ S_{\kappa}f_{\kappa}^{*}(p)\dfrac{\boldsymbol{\sigma}\cdot\boldsymbol{p}}{p}\end{pmatrix}\Phi_{\kappa}^{\mu}(\hat{\boldsymbol{p}}). \tag{5}$$

Assuming plane waves for the electron (treated in the extreme relativistic limit), the differential cross section for outgoing nucleon polarized $A(\vec{e},e'\vec{p})B$ reactions can be written in the laboratory system in the general form

$$\frac{d\sigma}{d\varepsilon_f d\Omega_f d\Omega_F} = \frac{E_F p_F}{(2\pi)^3}\sigma_M f_{rec}\omega_{\mu\nu}W^{\mu\nu}, \tag{6}$$

where σ_M is the Mott cross section, $\{\varepsilon_f,\Omega_f\}$ are the energy and solid angle corresponding to the scattered electron and $\Omega_F=(\theta_F,\phi_F)$ the solid angle for the outgoing proton. The factor f_{rec} is the usual recoil factor $f_{rec}^{-1}=|1-(E_F/E_B)(\boldsymbol{p}_B\cdot\boldsymbol{p}_F)/p_F^2|$, being $\boldsymbol{p}_B$ and E_B the momentum and energy of the residual nucleus, respectively. Finally, $\omega_{\mu\nu}$ is the familiar leptonic tensor that can be decomposed into its symmetric (helicity independent) and antisymmetric (helicity dependent) parts and $W^{\mu\nu}$ is the hadronic tensor which contains all of the hadronic dynamics of the process. The latter is defined from bilinear combinations of the one body nucleon current matrix elements given in Eq. (1), as

$$W^{\mu\nu} = \frac{1}{2j_b+1}\sum_{\mu_b} J^{\mu*}(\omega,\boldsymbol{q})J^{\nu}(\omega,\boldsymbol{q}). \tag{7}$$

The cross section can be also written in terms of hadronic responses by making use of the general properties of the leptonic tensor. For $(\vec{e},e'\vec{p})$ reactions with the incoming electron polarized and the final nucleon polarization also measured, a total set of 18 response functions contribute to the cross section. Its general expression is written in the form

$$\begin{aligned}\frac{d\sigma}{d\varepsilon_f d\Omega_f d\Omega_F} = \frac{E_F p_F}{(2\pi)^3}\sigma_M f_{rec}\frac{1}{2}\{&v_L(R^L + R_n^L\hat{S}_n) + v_T(R^T + R_n^T\hat{S}_n) + v_{TL}[(R^{TL} + R_n^{TL}\hat{S}_n)\cos\phi_F + (R_l^{TL}\hat{S}_l + R_s^{TL}\hat{S}_s)\sin\phi_F]\\ &+ v_{TT}[(R^{TT} + R_n^{TT}\hat{S}_n)\cos 2\phi_F + (R_l^{TT}\hat{S}_l + R_s^{TT}\hat{S}_s)\sin 2\phi_F] + h\{v_{TL'}[(R_l^{TL'}\hat{S}_l + R_s^{TL'}\hat{S}_s)\cos\phi_F + (R^{TL'} + R_n^{TL'}\hat{S}_n)\sin\phi_F]\\ &+ v_{T'}[R_l^{T'}\hat{S}_l + R_s^{T'}\hat{S}_s]\}\},\end{aligned} \tag{8}$$

where v_α are the usual electron kinematical factors [5,11] and $h=\pm 1$ is the incident electron helicity. The polarized and unpolarized nuclear response functions are constructed directly by taking the appropriate components of the hadronic tensor $W^{\mu\nu}$ (see Ref. [5] for their explicit expressions). The cross section dependence on the recoil nucleon polarization is specified by the components $\hat{S}_k$ $(k=l,n,s)$ of the ejected proton rest frame spin $(\boldsymbol{s}_F)_R$ along the directions: $\boldsymbol{l}=\boldsymbol{p}_F/p_F$, $\boldsymbol{n}=(\boldsymbol{q}\times\boldsymbol{p}_F)/|\boldsymbol{q}\times\boldsymbol{p}_F|$ and $\boldsymbol{s}=\boldsymbol{n}\times\boldsymbol{l}$.

To finish this section and in order to ease the analysis of the results, the cross section can be also expressed in terms of the usual polarization asymmetries, which are given as ratios between different classes of response functions,

$$\begin{aligned}\frac{d\sigma}{d\varepsilon_f d\Omega_f d\Omega_F} = \frac{\sigma_0}{2}[&1 + P_n\hat{S}_n + P_l\hat{S}_l + P_s\hat{S}_s\\ &+ h(A + P'_n\hat{S}_n + P'_l\hat{S}_l + P'_s\hat{S}_s)],\end{aligned} \tag{9}$$

with σ_0 the unpolarized cross section, A the electron analyzing power, and P_k (P'_k) the induced (transferred) polarizations.

Factorization and effective momentum approximation

In nonrelativistic PWIA, the $(e,e'p)$ unpolarized cross section factorizes in the form

$$\left(\frac{d\sigma}{d\varepsilon_f d\Omega_f d\Omega_F}\right)^{PWIA} = E_F p_F f_{rec}\sigma_{ep}N_{NR}(\boldsymbol{p}_m), \tag{10}$$

where σ_{ep} is the bare electron-proton cross section usually taken as σ_{cc1} (or σ_{cc2}) of de Forest [23], and $N_{NR}(\boldsymbol{p}_m)$ is the *nonrelativistic momentum distribution* that represents the probability of finding a proton in the target nucleus with missing momentum $\boldsymbol{p}_m$, compatible with the kinematics of the reaction. It is well known that the factorized result in Eq. (10) comes from an oversimplified description of the reaction mechanism. FSI, as well as Coulomb distortion of the electron wave functions, destroys in general factorization. In fact, most current descriptions of exclusive $(e,e'p)$ reactions involve unfactorized calculations. However, the simplicity of the factorized result makes it very useful to analyze and interpret electron scattering observables in terms of single particle properties of bound nucleons. Therefore it is common to quote *experimental reduced cross section or effective momentum distribution* on the basis of the experimental unpolarized cross section as

$$\rho^{exp}(\boldsymbol{p}_m) = \frac{(d\sigma/d\varepsilon_f d\Omega_f d\Omega_F)^{exp}}{E_F p_F f_{rec}\sigma_{ep}}. \tag{11}$$

A similar expression can be used for the theoretical reduced cross section,

$$\rho^{th}(\boldsymbol{p}_m) = \frac{(d\sigma/d\varepsilon_f d\Omega_f d\Omega_F)^{th}}{E_F p_F f_{rec}\sigma_{ep}}, \tag{12}$$

constructed from the the theoretical unpolarized $(e,e'p)$ cross section, independently of whether it is calculated within a relativistic or nonrelativistic formalism. We will say that the factorization property is satisfied by $\rho^{th}(\boldsymbol{p}_m)$ when the theoretical unpolarized cross section factors out exactly σ_{ep}, and then, the theoretical reduced cross section does not depend on it.

As we will demonstrate later in this paper, factorization is not a property exclusive of the nonrelativistic PWIA approach. It is well known that, due to the negative energy components of the bound proton wave function, factorization is not satisfied even in RPWIA [18]. However, if we neglect the contribution from the negative energy components, the unpolarized cross section factorizes to a similar expression as in Eq. (10).

Starting from a fully relativistic calculation of the nuclear current, in what follows we explore the most general conditions under which factorization is recovered. First, it is important to note that in order to extract the elementary cross section "σ_{ep}" from the general relativistic theory (RDWIA), the upper and lower components of the relativistic wave functions that enter in Eq. (1) must be forced to satisfy the "free" relationship with momenta determined by asymptotic kinematics at the nucleon vertex, that is

$$\psi_{down}(\boldsymbol{p}) = \frac{\boldsymbol{\sigma}\cdot\boldsymbol{p}_{as}}{E_{as}+M}\psi_{up}(\boldsymbol{p}) \tag{13}$$

with $E_{as}=\sqrt{\boldsymbol{p}_{as}^2+M^2}$ and $\boldsymbol{p}_{as}$ the asymptotic momentum corresponding to each nucleon. In what follows we discuss this condition (13) in the nonrelativistic language.

The nonrelativistic formalism is based on bispinors $\chi(\boldsymbol{p})$ solutions of Schrödinger-like equations. Generally, the nonrelativistic formalism can be analyzed using the following semirelativistic four-spinor

$$\psi^{SR}(\boldsymbol{p}) = \frac{1}{\sqrt{N}}\begin{pmatrix}\chi(\boldsymbol{p})\\ \dfrac{\boldsymbol{\sigma}\cdot\boldsymbol{p}}{E+M}\chi(\boldsymbol{p})\end{pmatrix}, \tag{14}$$

to be introduced in Eq. (1) in order to calculate a relativisticlike nucleon current amplitude. In this way the relativistic kinematics is fully taken into account and no expansions in p/M are needed. The one body nucleon current matrix element takes then the following form:

$$J^{\mu}(\omega,\boldsymbol{q}) = \int d\boldsymbol{p}\,\chi_F^{s_F\dagger}(\boldsymbol{p}+\boldsymbol{q})\hat{J}^{\mu}_{eff}(\boldsymbol{p},\boldsymbol{q})\chi^{\mu_b}_{j_b}(\boldsymbol{p}), \tag{15}$$

with $\hat{J}^{\mu}_{eff}(\boldsymbol{p},\boldsymbol{q})$ now an effective (2×2) current operator that occurs between bispinor wave functions $\chi_F^{s_F}$ $(\chi^{\mu_b}_{j_b})$ for the outgoing (bound) nucleon respectively.

The calculation of the nuclear amplitude using four-spinors like the one written in Eq. (14), implies removal of the enhancement of the lower components that is present in the four-spinors of Eqs. (2) and (4). This is a well known fact present in nonrelativistic calculations, but this alone is not enough to get factorization. It is also required the use of exactly the same nuclear current operator as in a free electron-proton scattering. In Eq. (15) then, the nontruncated effective current operator must be evaluated at the asymptotic momentum values, leading to

$$J^{\mu}(\omega,\boldsymbol{q}) = \int d\boldsymbol{p}\,\chi_F^{s_F\dagger}(\boldsymbol{p}+\boldsymbol{q})\hat{J}^{\mu}_{eff}(\boldsymbol{p}_F-\boldsymbol{q},\boldsymbol{q})\chi^{\mu_b}_{j_b}(\boldsymbol{p}). \tag{16}$$

One can show that this condition is implicit in one of the necessary assumptions introduced in Ref. [3] to recover factorization in the nonrelativistic case.

In a relativistic calculation, the assumptions written in Eq. (13) set up the so-called effective momentum approximation with no scalar and vector terms (EMA-noSV),[1] originally introduced by Kelly [22], to which we will refer in what follows as EMA. The EMA approximation in the relativistic framework, or the nonrelativistic calculation based on Eq. (16), are essentially the same conditions which are necessary to recover factorization, in either formalism. These conditions are necessary but not sufficient and in what follows, we concentrate on the EMA case to study additional assumptions needed to obtain factorization.

[1]The factorization property could be also analyzed within the framework of the asymptotic projection approach (see Refs. [9,11,16] for details).

In EMA, the bound nucleon wave function in momentum space is given by

$$\psi^{\mu_b\ EMA}_{\kappa_b}(\boldsymbol{p}) = (-i)^{\ell_b}\begin{pmatrix} g_{\kappa_b}(p)\\ \dfrac{\boldsymbol{\sigma}\cdot\boldsymbol{p}_I}{E_I+M}g_{\kappa_b}(p)\end{pmatrix}\Phi^{\mu_b}_{\kappa_b}(\hat{\boldsymbol{p}}) \tag{17}$$

with $E_I=\sqrt{\boldsymbol{p}_I^2+M^2}$ and $\boldsymbol{p}_I=\boldsymbol{p}_F-\boldsymbol{q}$. Likewise the outgoing relativistic distorted wave function in Eq. (5) becomes

$$\psi^{\mu\ EMA}_{\kappa}(\boldsymbol{p}) = (-i)^{\ell}\begin{pmatrix} g^*_{\kappa}(p)\\ \dfrac{\boldsymbol{\sigma}\cdot\boldsymbol{p}_F}{E_F+M}g^*_{\kappa}(p)\end{pmatrix}\Phi^{\mu}_{\kappa}(\hat{\boldsymbol{p}}). \tag{18}$$

Introducing these expressions into the equation of the one body nucleon current matrix element [Eq. (1)], we get

$$\begin{aligned} J^{\mu}_{EMA} &= \sum_{sh}[\overline{u}(\boldsymbol{p}_F,s)\hat{J}^{\mu}u(\boldsymbol{p}_I,h)]\sum_{\kappa\mu m}\left\langle \ell m\frac{1}{2}s_F|j\mu\right\rangle Y^{m*}_{\ell}(\hat{\boldsymbol{p}}_F)\\ &\times\sum_{m_{\ell_b}m_{\ell}}\left\langle \ell_b m_{\ell_b}\frac{1}{2}h|j_b\mu_b\right\rangle\left\langle \ell m_{\ell}\frac{1}{2}s|j\mu\right\rangle U^{\kappa\ m_{\ell}}_{\kappa_b\ m_{\ell_b}}(\boldsymbol{p}_F,\boldsymbol{q})\\ &\equiv\sum_{sh}J^{\mu}_{bare}(\boldsymbol{p}_F s,\boldsymbol{p}_I h)A^{\mu_b}_{sh}(\boldsymbol{p}_F,\boldsymbol{q}), \end{aligned} \tag{19}$$

where we have written both nucleon wave functions in terms of free positive energy Dirac spinors and we have introduced the bare nucleon current matrix element

$$J^{\mu}_{bare}(\boldsymbol{p}_F s,\boldsymbol{p}_I h) = \overline{u}(\boldsymbol{p}_F,s)\hat{J}^{\mu}u(\boldsymbol{p}_I,h), \tag{20}$$

with the term $U^{\kappa\ m_{\ell}}_{\kappa_b\ m_{\ell_b}}(\boldsymbol{p}_F,\boldsymbol{q})$ given by

$$\begin{aligned} U^{\kappa\ m_{\ell}}_{\kappa_b\ m_{\ell_b}} &= \frac{8\pi M}{\sqrt{2E_F(E_I+M)}}(-i)^{\ell_b}\int d\boldsymbol{p}\,g_{\kappa_b}(p)g^*_{\kappa}(|\boldsymbol{p}+\boldsymbol{q}|)\\ &\times Y^{m_{\ell_b}}_{\ell_b}(\hat{\boldsymbol{p}})Y^{m_{\ell}*}_{\ell}(\widehat{\boldsymbol{p}+\boldsymbol{q}})e^{i\delta_{\kappa}}, \end{aligned} \tag{21}$$

and the amplitude

$$\begin{aligned} A^{\mu_b}_{sh}(\boldsymbol{p}_F,\boldsymbol{q}) &= \sum_{\kappa\mu m}\left\langle \ell m\frac{1}{2}s_F|j\mu\right\rangle Y^{m*}_{\ell}(\hat{\boldsymbol{p}}_F)\sum_{m_{\ell_b}m_{\ell}}\left\langle \ell_b m_{\ell_b}\frac{1}{2}h|j_b\mu_b\right\rangle\\ &\times\left\langle \ell m_{\ell}\frac{1}{2}s|j\mu\right\rangle U^{\kappa\ m_{\ell}}_{\kappa_b\ m_{\ell_b}}(\boldsymbol{p}_F,\boldsymbol{q}). \end{aligned} \tag{22}$$

The result in Eq. (19) defines the nucleon current in EMA, and is our starting point for the analysis of the conditions that may lead to factorized observables. Notice that J^{μ}_{EMA} involves a sum over initial and final spin projections $(s,\ h)$ of the bare nucleon current, times an amplitude that depends on the bound and ejected nucleon wave functions. Factorization in J^{μ}_{EMA} occurs if $A^{\mu_b}_{sh}(\boldsymbol{p}_F,\boldsymbol{q})$ does not depend on the spin variables s and h.

Before entering into a detailed discussion of the observables, it is important to stress again that factorization may only be achieved assuming EMA and/or asymptotic projection, i.e., neglecting dynamical enhancement of the lower components in the nucleon wave functions. This is *a priori* assumed within some nonrelativistic calculations.

III. ANALYSIS OF OBSERVABLES WITHIN EMA

In this section we investigate the conditions that lead to factorization of polarized and unpolarized observables. Response functions, transverse-longitudinal asymmetry, electron analyzing power, as well as induced and transferred polarizations are examined. The analysis is made directly at the level of the hadronic tensor which, within the EMA approach, can be written in the following way:

$$\begin{aligned} W^{\mu\nu}_{EMA} &= \frac{1}{2j_b+1}\sum_{\mu_b}(J^{\mu}_{EMA})^{*}J^{\nu}_{EMA} \\ &= \sum_{ss'}\sum_{hh'}[J^{\mu}_{bare}(\boldsymbol{p}_F s,\boldsymbol{p}_I h)]^{*}J^{\nu}_{bare}(\boldsymbol{p}_F s',\boldsymbol{p}_I h') \\ &\quad\times\frac{1}{2j_b+1}\sum_{\mu_b}[A^{\mu_b}_{sh}(\boldsymbol{p}_F,\boldsymbol{q})]^{*}A^{\mu_b}_{s'h'}(\boldsymbol{p}_F,\boldsymbol{q}). \end{aligned} \tag{23}$$

Note that in Eq. (23) s,s' are the spin variables corresponding to the outgoing nucleon, while h,h' correspond to the bound nucleon.

In order to simplify the analysis that follows, the general expression of the hadronic tensor can be written in a more compact form as

$$W^{\mu\nu}_{EMA}=\sum_{ss'}\sum_{hh'}\mathcal{W}^{\mu\nu}_{ss',hh'}X^{s_F}_{ss',hh'}(\boldsymbol{p}_F,\boldsymbol{q}), \tag{24}$$

where we have introduced a general bare-nucleon tensor $\mathcal{W}^{\mu\nu}_{ss',hh'}$,

$$\begin{aligned} \mathcal{W}^{\mu\nu}_{ss',hh'} &= (J^{\mu}_{bare})^{*}J^{\nu}_{bare} \\ &= [\overline{u}(\boldsymbol{p}_F,s)\hat{J}^{\mu}u(\boldsymbol{p}_I,h)]^{*}[\overline{u}(\boldsymbol{p}_F,s')\hat{J}^{\nu}u(\boldsymbol{p}_I,h')], \end{aligned} \tag{25}$$

and a general spin dependent momentum distribution function $X^{s_F}_{ss',hh'}$,

$$\begin{aligned} X^{s_F}_{ss',hh'}(\boldsymbol{p}_F,\boldsymbol{q}) &= \frac{1}{2j_b+1}\sum_{\mu_b}[A^{\mu_b}_{sh}(\boldsymbol{p}_F,\boldsymbol{q})]^{*}A^{\mu_b}_{s'h'}(\boldsymbol{p}_F,\boldsymbol{q}) \\ &= \frac{1}{2j_b+1}\sum_{\mu_b}\sum_{\kappa\mu m}\sum_{\kappa'\mu' m'}\left\langle \ell m\frac{1}{2}s_F|j\mu\right\rangle \\ &\quad\times\left\langle \ell' m'\frac{1}{2}s_F|j'\mu'\right\rangle Y^{m}_{\ell}(\hat{\boldsymbol{p}}_F)Y^{m'*}_{\ell'}(\hat{\boldsymbol{p}}_F) \\ &\quad\times\sum_{m_{\ell_b}m_{\ell}m'_{\ell_b}m'_{\ell}}\left\langle \ell_b m_{\ell_b}\frac{1}{2}h|j_b\mu_b\right\rangle\left\langle \ell m_{\ell}\frac{1}{2}s|j\mu\right\rangle \\ &\quad\times\left\langle \ell_b m'_{\ell_b}\frac{1}{2}h'|j_b\mu_b\right\rangle\left\langle \ell' m'_{\ell}\frac{1}{2}s'|j'\mu'\right\rangle \\ &\quad\times U^{\kappa\ m_{\ell}*}_{\kappa_b\ m_{\ell_b}}(\boldsymbol{p}_F,\boldsymbol{q})U^{\kappa'\ m_{\ell}}_{\kappa_b\ m'_{\ell_b}}(\boldsymbol{p}_F,\boldsymbol{q}). \end{aligned} \tag{26}$$

Making use of general symmetry properties (see Appendix A), the bare-nucleon tensor in Eq. (25) can be decomposed into terms which are symmetric and antisymmetric under interchange of μ and ν. Each of these terms shows a different dependence on the spin variables: ss' and/or hh'. Explicitly, the bare nucleon tensor can be written in the form

$$\mathcal{W}^{\mu\nu}_{ss',hh'}=\mathcal{S}^{\mu\nu}\ \delta_{ss'}\ \delta_{hh'}+\mathcal{A}^{\mu\nu}_{hh'}\ \delta_{ss'}+\mathcal{A}^{\mu\nu}_{ss'}\ \delta_{hh'}+\mathcal{S}^{\mu\nu}_{ss',hh'}, \tag{27}$$

where S ($\mathcal{A}$) refers to symmetric (antisymmetric) tensors. Notice that the first (symmetric) term in Eq. (27) does not depend on the initial bound neither on the final outgoing nucleon spin variables; the antisymmetric second (third) term depends solely on the initial (final) spin projections; finally, the fourth (symmetric) term presents dependence on both initial and final nucleon spin projections simultaneously. This bare-nucleon tensor would lead to the σ_{ep} cross section in Eq. (10).

The general result for the bare nucleon tensor given in Eq. (28) constitutes the starting point for the analysis of factorization for polarized as well as unpolarized observables. In what follows we explore the specific conditions, linked to the spin dependence in the problem, that lead to factorized results. We investigate separately the role played by the dependence on the initial and/or final nucleon spin variables. As we show in next subsections, the factorization property at the level of spin-averaged squared matrix elements is intimately connected with the spin dependence: a bound nucleon in an s-wave or, in general, no spin-orbit coupling effects on the radial nucleon wave functions, may lead for some specific observables to exactly factorized results. As it is clear from the analogy between Eq. (16) and Eq. (1) with the input from Eq. (13), the analysis of spin dependence here and in what follows is also valid for the nonrelativistic case.

A. No spin-orbit in the initial state

The general expression of $X^{s_F}_{ss',hh'}$ (26) is greatly simplified for no spin-orbit in the initial state or, more generally in LS coupling. For instance in the case of nucleon knockout from s-shells the orbital angular momentum $\ell_b=0$ and the spin dependent momentum distribution is simply given by

$$X^{s_F}_{ss',hh'}(\boldsymbol{p}_F,\boldsymbol{q})=N^{s_F}_{ss'}(\boldsymbol{p}_F,\boldsymbol{q})\ \delta_{hh'}, \tag{28}$$

with

$$\begin{aligned} N^{s_F}_{ss'}(\boldsymbol{p}_F,\boldsymbol{q}) &= \frac{1}{2j_b+1}\sum_{\kappa\mu m}\sum_{\kappa' m'}\left\langle \ell m\frac{1}{2}s_F|j\mu\right\rangle \\ &\quad\times\left\langle \ell' m'\frac{1}{2}s_F|j'\mu'\right\rangle Y^{m}_{\ell}(\hat{\boldsymbol{p}}_F)Y^{m'*}_{\ell'}(\hat{\boldsymbol{p}}_F) \\ &\quad\times\sum_{m_{\ell}m'_{\ell}}\left\langle \ell m_{\ell}\frac{1}{2}s|j\mu\right\rangle \\ &\quad\times\left\langle \ell' m'_{\ell}\frac{1}{2}s'|j'\mu'\right\rangle U^{\kappa\ m'_{\ell}*}_{-10}(\boldsymbol{p}_F,\boldsymbol{q})U^{\kappa'\ m_{\ell}}_{-10}(\boldsymbol{p}_F,\boldsymbol{q}). \end{aligned} \tag{29}$$

In the case of no spin-orbit coupling with $\ell_b\neq 0$ waves, a similar reduction to Eq. (28) follows after summation of the spin dependent momentum distribution X on $j_b=\ell_b\pm 1/2$.

Making use of Eqs. (27) and (28) the hadronic tensor in EMA becomes

$$W^{\mu\nu}_{EMA} = \sum_{ss'} N^{s_F}_{ss'} \left[\sum_{h} \mathcal{W}^{\mu\nu}_{ss',hh} \right] = \sum_{ss} N^{s_F}_{ss'} [S^{\mu\nu}\delta_{ss'} + \mathcal{A}^{\mu\nu}_{ss'}] = S^{\mu\nu} \sum_{s} N^{s_F}_{ss} + \sum_{ss'} N^{s_F}_{ss'} \mathcal{A}^{\mu\nu}_{ss'}. \quad (30)$$

From this result it clearly emerges that those responses coming from the symmetric tensor $\mathcal{S}^{\mu\nu}$ factorize, while the ones coming from the antisymmetric part do not. Let us describe more precisely what factorization really means in this situation.

First, note that the momentum distribution function $\Sigma_s N^{s_F}_{ss}$ that multiplies the symmetric tensor depends on the outgoing nucleon spin s_F. In the case when recoil nucleon polarization is not measured, an extra sum in s_F has to be carried out and hence the momentum distribution, which is independent of s_F, gives rise to the unpolarized responses R^L, R^T, R^{TL} and R^{TT} in Eq. (8). On the other hand, if the spin of the outgoing proton is measured via a polarimeter placed along a fixed direction ($\boldsymbol{n}$, $\boldsymbol{l}$ or $\boldsymbol{s}$), the momentum distribution, now dependent on the final spin, contributes to the induced polarized responses: R^L_n, R^T_n, $R^{TL}_{n,l,s}$ and $R^{TT}_{n,l,s}$. Hence, in the case of no spin-orbit coupling in the initial bound state, both types of responses (unpolarized and induced polarized) factorize, but each kind of response factorizes with a different momentum distribution function. Then, the induced polarization asymmetries P_k ($k=l,n,s$), which are basically given by the ratio between the induced polarized responses R^α_k and the unpolarized ones R^α, will differ from the bare result. On the contrary, the momentum distribution functions cancel when taking a ratio between two responses of the same kind, i.e., a ratio between two induced polarized responses along a specific direction, or a ratio between two unpolarized responses. Therefore such ratios would coincide with the bare results. This property can be expressed in the general form

$$\frac{R^\alpha_k}{R^\beta_k} = \frac{R^\alpha}{R^\beta} = \frac{\mathcal{R}^\alpha}{\mathcal{R}^\beta}, \quad (31)$$

where $\alpha,\beta=L,T,TL$ or TT and $k=l,n,s$ fixes the recoil nucleon polarization direction. The functions $\mathcal{R}^{\alpha,\beta}$ represent the bare-nucleon responses, also usually named single-nucleon responses [21]. The result in Eq. (31) explains also why the A_{TL} asymmetry, which is obtained from the difference of electron unpolarized cross sections measured at $\phi_F = 0^\circ$ and $\phi_F = 180^\circ$ divided by the sum, is identical to the bare asymmetry in this case. In terms of response functions we may write

$$A_{TL} = \frac{v_{TL}R^{TL}}{v_L R^L + v_T R^T + v_{TT} R^{TT}} = \frac{v_{TL}\mathcal{R}^{TL}}{v_L \mathcal{R}^L + v_T \mathcal{R}^T + v_{TT} \mathcal{R}^{TT}} = A^{bare}_{TL}. \quad (32)$$

To complete the discussion, we note that the electron analyzing power and transferred polarization asymmetries involve responses coming from the antisymmetric part of the tensor (30), which do not factorize, divided by unpolarized responses obtained from the symmetric tensor term. Therefore the behavior of A and P'_k will differ from the bare one. The amount of discrepancy between the factorized and unfactorized calculations of different observables is discussed in Sec. V.

B. No spin-orbit in the final state

Let us consider now the case of no spin-orbit coupling effects on the radial wave function of the outgoing proton. In this case neither δ_κ nor g_κ in Eqs. (4) and (18) depend on j. After some algebra (see Appendix B for details), this condition leads to $s=s'=s_F$ in the bare-nucleon tensor, and therefore the momentum distribution depends only on the hh' spin variables of the initial nucleon. The hadronic tensor is then given by

$$W^{\mu\nu}_{EMA} = \sum_{hh'} \mathcal{W}^{\mu\nu}_{s_F s_F,hh'} \widetilde{N}_{hh'}(\boldsymbol{p}_F, \boldsymbol{q}), \quad (33)$$

where the momentum distribution function $\widetilde{N}_{hh'}(\boldsymbol{p}_F,\boldsymbol{q})$ is defined in Eq. (B6) of Appendix B. Using the decomposition in Eq. (27), we can write the following expression:

$$W^{\mu\nu}_{EMA} = [\mathcal{S}^{\mu\nu} + \mathcal{A}^{\mu\nu}_{s_F s_F}] \sum_{h} \widetilde{N}_{hh} + \sum_{hh'} [\mathcal{S}^{\mu\nu}_{s_F s_F,hh'} + \mathcal{A}^{\mu\nu}_{hh'}] \widetilde{N}_{hh'}. \quad (34)$$

The analysis of how polarized or unpolarized responses behave with respect to factorization emerges straightforwardly from Eq. (34). Let us discuss each case separately:

(i) Unpolarized responses: R^L, R^T, R^{TL} and R^{TT}. They do not depend on spin and come from the symmetric part of the tensor, i.e., they are given by $\mathcal{S}^{\mu\nu}\Sigma_h \widetilde{N}_{hh}$, and hence factorize exactly. This result coincides with that one obtained in the nonrelativistic study of Ref. [3].

(ii) Transferred polarization responses: $R^{T'}_{l,s}$ and $R^{TL'}_{l,s,n}$. They come from the antisymmetric part of the tensor and depend on the final proton spin polarization, i.e., $\mathcal{A}^{\mu\nu}_{s_F s_F} \Sigma_h \widetilde{N}_{hh}$, in exactly the same form as displayed in Eq. (27). Consequently, these responses also factorize.

(iii) Fifth response $R^{TL'}$. It comes from the antisymmetric part of the tensor and does not depend on the recoil nucleon spin, i.e., it is given by $\Sigma_{hh'} \widetilde{N}_{hh'} \mathcal{A}^{\mu\nu}_{hh'}$ and clearly does not factorize.

(iv) Induced polarized responses: R^L_n, R^T_n, $R^{TL}_{n,l,s}$ and $R^{TT}_{n,l,s}$. They come from the symmetric tensor part and depend explicitly on the spin polarization of the outgoing proton, i.e., they are constructed from $\Sigma_{hh'} \widetilde{N}_{hh'} \mathcal{S}^{\mu\nu}_{s_F s_F,hh'}$, and consequently do not factorize.

Once the behavior of the response functions is established, the asymmetries and polarization ratios can be easily analyzed. The case of A_{TL}, which only depends on the unpolarized responses, reduces to A^{bare}_{TL} [see Eq. (32)]. A similar

comment applies also to the transferred nucleon polarizations P'_l, P'_s, and P'_n. Notice that the momentum distribution function involved in the unpolarized and transferred polarized responses is the same and hence, it cancels when forming the polarization ratios. The electron analyzing power A and induced asymmetries P_k, given in terms of responses which do not factorize, should differ from the bare calculations.

As a particular case of no spin-orbit in the final nucleon wave function, it is worth to explore the plane wave limit for the outgoing nucleon. In this case [see Eq. (B8) in Appendix B], the momentum distribution $\widetilde{N}^{PW}_{hh'}$ is diagonal and independent on h, thus the fifth response $R^{TL'}$ vanishes since $\Sigma_h \mathcal{A}^{\mu\nu}_{hh}=0$. Similarly, the induced polarization responses do not contribute because $\Sigma_h \mathcal{S}^{\mu\nu}_{s_F s_F,hh}=0$.

C. No spin-orbit in both initial and final states

To finish with this analysis, let us consider the case of no spin-orbit coupling in the initial nor in the final state. In this situation, factorization already comes out at the level of the nuclear current matrix element. Note that $\ell_b=0$ in Eq. (B4) of Appendix B, leads to $h=\mu_b$ and the matrix element simply reads

$$J^{\mu}_{EMA}=\overline{u}(\boldsymbol{p}_F,s_F)\hat{J}^{\mu}u(\boldsymbol{p}_I,\mu_b)\ U^0_{-1}(\boldsymbol{p}_F,\boldsymbol{q}), \tag{35}$$

where U^0_{-1} is defined in Eq. (B5). This result resembles the situation occurring in the free case. From the current (35) the hadronic tensor can be written in the form

$$W^{\mu\nu}_{EMA}=\frac{1}{2}|U^0_{-1}(\boldsymbol{p}_F,\boldsymbol{q})|^2\sum_{\mu_b}\mathcal{W}^{\mu\nu}_{s_F s_F,\mu_b\mu_b}$$
$$=\frac{1}{2}|U^0_{-1}(\boldsymbol{p}_F,\boldsymbol{q})|^2(\mathcal{S}^{\mu\nu}+\mathcal{A}^{\mu\nu}_{s_F s_F}). \tag{36}$$

Then all responses (polarized and unpolarized) factorize with the same momentum distribution. Note also that the whole dependence on the nucleon polarization s_F is contained in the antisymmetric tensor. This implies that the polarized induced responses must be zero. Furthermore, since $\Sigma_{s_F}\mathcal{A}^{\mu\nu}_{s_F s_F}=0$ the unpolarized fifth response $R^{TL'}$ also vanishes.

IV. REDUCED CROSS SECTIONS AND MOMENTUM DISTRIBUTIONS

Starting from a shell model approach, the relativistic (vector) momentum distribution is defined as follows:

$$N(p_I)=\frac{1}{2j_b+1}\sum_{\mu_b}\psi^{\mu_b\dagger}_{\kappa_b}(\boldsymbol{p}_I)\psi^{\mu_b}_{\kappa_b}(\boldsymbol{p}_I)=\frac{1}{4\pi}[g^2_{\kappa_b}(p_I)+f^2_{\kappa_b}(p_I)]. \tag{37}$$

Using the EMA approximation means projecting out the negative energies components of the bound proton wave function, obtaining then the relativistic EMA momentum distribution:

$$N^{EMA}(\boldsymbol{p}_I)=\frac{1}{2j_b+1}\sum_{\mu_b}\psi^{\mu_b EMA\dagger}_{\kappa_b}(\boldsymbol{p}_I)\psi^{\mu_b EMA}_{\kappa_b}(\boldsymbol{p}_I)$$
$$=\frac{1}{4\pi}\frac{2E_I}{E_I+M}g^2_{\kappa_b}(p_I), \tag{38}$$

this expression reduces to the nonrelativistic momentum distribution in the proper limit because of its lack of contribution from negative energies.

In general, in a nonrelativistic formalism, the momentum distribution is defined from bispinors $\chi^{\mu_b}_{j_b}(\boldsymbol{r})$, solutions of Schrödinger-like equation:

$$N_{NR}(p_I)=\frac{1}{2j_b+1}\sum_{\mu_b}\chi^{\mu_b\dagger}_{j_b}(\boldsymbol{p}_I)\chi^{\mu_b}_{j_b}(\boldsymbol{p}_I), \tag{39}$$

with $\chi^{\mu_b}_{j_b}(\boldsymbol{p}_I)$ the Fourier transform of $\chi^{\mu_b}_{j_b}(\boldsymbol{r})$,

$$\chi^{\mu_b}_{j_b}(\boldsymbol{p}_I)=\frac{1}{(2\pi)^{3/2}}\int d\boldsymbol{r}e^{-i\boldsymbol{p}_I\cdot\boldsymbol{r}}\chi^{\mu_b}_{j_b}(\boldsymbol{r}). \tag{40}$$

Now, in nonrelativistic PWIA, the wave function for the ejected proton in the $\boldsymbol{r}$-space is

$$\chi^{s_F PW}_F(\boldsymbol{r})=e^{i\boldsymbol{p}_F\cdot\boldsymbol{r}}\chi^{s_F}_{1/2}, \tag{41}$$

and looking at the the Fourier transform in Eq. (40), it is natural to define a nonrelativistic distorted wave amplitude as follows:

$$\chi_{DW}(\boldsymbol{p}_F,\boldsymbol{q})\equiv\frac{1}{(2\pi)^{3/2}}\int d\boldsymbol{r}\chi^{s_F\dagger}_F(\boldsymbol{r})e^{i\boldsymbol{q}\cdot\boldsymbol{r}}\chi^{\mu_b}_{j_b}(\boldsymbol{r}). \tag{42}$$

Two observations are worth mentioning:

(1) $\chi_{DW}(\boldsymbol{p}_F,\boldsymbol{q})$ is an amplitude, not a bispinor.

(2) If the final proton wave function is a plane wave, the following relationship is satisfied:

$$\sum_{s_F}|\chi_{PW}(\boldsymbol{p}_F,\boldsymbol{q})|^2=\chi^{\mu_b\dagger}_{j_b}(\boldsymbol{p}_I)\chi^{\mu_b}_{j_b}(\boldsymbol{p}_I). \tag{43}$$

So, we can define a nonrelativistic distorted momentum distribution

$$\rho^{NR}_{DW}(\boldsymbol{p}_F,\boldsymbol{q})=\frac{1}{2j_b+1}\sum_{\mu_b}\sum_{s_F}|\chi_{DW}(\boldsymbol{p}_F,\boldsymbol{q})|^2, \tag{44}$$

that takes into account FSI, and has the property that we recover the nonrelativistic momentum distribution in Eq. (39) in the plane wave limit.

Let us generalize the above expression to the relativistic case. We request that we recover from it the relativistic EMA momentum distribution of Eq. (38) when there is not FSI and the initial wave function is evaluated within EMA. For that purpose we define a relativistic distorted wave amplitude,

$$\psi_{DW}(\boldsymbol{p}_F,\boldsymbol{q})\equiv\frac{K}{(2\pi)^{3/2}}\int d\boldsymbol{r}\psi^{s_F\dagger}_F(\boldsymbol{r})e^{i\boldsymbol{q}\cdot\boldsymbol{r}}\psi^{\mu_b}_{\kappa_b}(\boldsymbol{r})$$
$$=\frac{K}{(2\pi)^{3/2}}\int d\boldsymbol{p}\psi^{s_F\dagger}_F(\boldsymbol{p}+\boldsymbol{q})\psi^{\mu_b}_{\kappa_b}(\boldsymbol{p}) \tag{45}$$

with $K=\sqrt{(2E_IE_F)/(E_IE_F+\boldsymbol{p}_I\cdot\boldsymbol{p}_F+M^2)}$, so that the relativistic

distorted momentum distribution is given by this amplitude squared after sum and average over initial and final spins,

$$\rho_{DW}(\boldsymbol{p}_F,\boldsymbol{q}) = \frac{1}{2j_b+1}\sum_{\mu_b}\sum_{s_F}|\psi_{DW}(\boldsymbol{p}_F,\boldsymbol{q})|^2. \qquad (46)$$

It is easy to check that $\rho_{DW}(\boldsymbol{p}_F,\boldsymbol{q})$ coincides with the relativistic EMA momentum distribution Eq. (38), when one takes EMA approximation for the initial wave function and the plane wave limit for the final one,

$$\rho_{PW}^{EMA}(\boldsymbol{p}_F,\boldsymbol{q}) = N^{EMA}(p_I). \qquad (47)$$

It is also important to remark that $\rho_{DW}(\boldsymbol{p}_F,\boldsymbol{q})$ coincides with the corresponding reduced cross section of Eq. (12) whenever there is factorization.

V. NUMERICAL RESULTS

To show quantitatively the effects introduced by the different approaches to the general description of $(\vec{e},e'\vec{p})$ reactions, we compare our fully RDWIA calculations with the EMA results, exploring also the effects introduced by the spin variables in the initial and final nucleon states. The results presented in this section illustrate and reinforce the conclusions reached in the preceding sections concerning the factorization properties.

Guided by the factorization properties one may focus on two different aspects in the analysis of observables.

(1) On the one hand, one may factor out the elementary electron-proton electromagnetic cross section, in order to isolate and investigate nuclear properties like momentum distributions. To the extent that factorization holds the reduced cross section will follow the momentum distribution. In the first part of this section we compare factorized and unfactorized results for the reduced cross section to the momentum distribution. We show how the different ingredients that break factorization may obscure the extraction of momentum distributions. First of all, we note that since FSI modify the response of the ejected nucleon, it is more adequate to compare reduced cross sections with distorted momentum distributions (as defined in the previous section). This is done in Fig. 1 that we discuss below.

(2) On the other hand, one may take ratios between observables to cancel out the dependence on the momentum distribution, in order to isolate and investigate intrinsic nucleon properties in the nuclear medium, like nucleon form factors.

In Fig. 1 we present reduced cross sections at quasielastic kinematics for three cases: complete RDWIA approach (solid line), EMA (dashed line), and EMA with no spin dependence in the final state, referred to as EMA-noLS (dotted line). We also show by a thin solid line the distorted momentum distributions [ρ_{DW}, Eq. (46)] which are equivalent to what one would obtain from a factorized approach to RDWIA. Note that up to $|p_m|$ of around 250 MeV/c, the factorized approach ρ_{DW} follows reasonably well the full calculation. Actually in this p_m range, EMA and EMA-noLS are also reasonable approximations to the complete calculation. However, at $|p_m|>250$ MeV/c the full approach produces more reduced cross section for $p_m<0$ than for $p_m>0$, leading to a much larger asymmetry in this region as we would see in Fig. 2. We also note that differences between complete RDWIA reduced cross section and ρ_{DW} (hence deviations

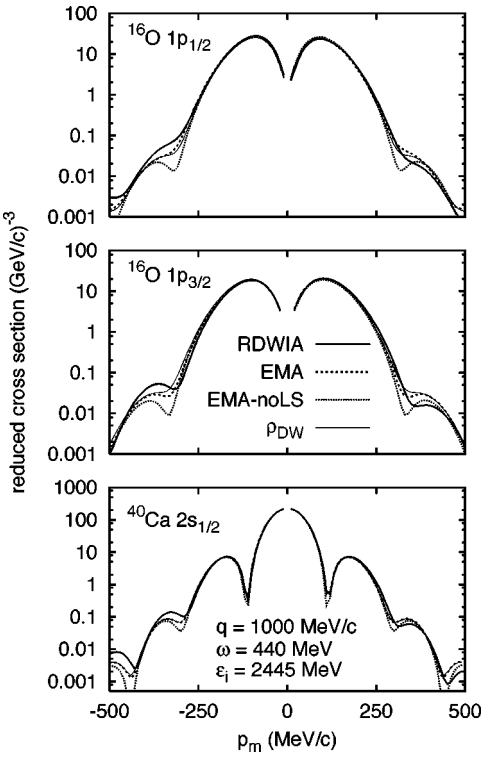

FIG. 1. Reduced cross section for proton knockout from $1p_{1/2}$ (upper panel) and $1p_{3/2}$ (middle panel) in ^{16}O and from $2s_{1/2}$ in ^{40}Ca (lower panel). RDWIA calculations (solid line) are compared to EMA (short-dashed line) and EMA-noLS (dotted line) results. The corresponding relativistic distorted wave momentum distribution is also plotted (thin solid line). Negative (positive) p_m values correspond to $\phi_F=0°$ (180°), respectively.

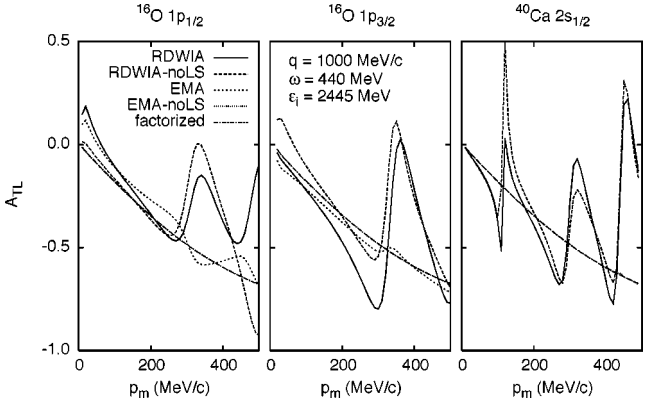

FIG. 2. A_{TL} asymmetry for proton knockout from $1p_{1/2}$ (left panel) and $1p_{3/2}$ (middle panel) in ^{16}O and from $2s_{1/2}$ in ^{40}Ca (right panel). RDWIA calculations (solid line) are compared to RDWIA-noLS (dashed line), EMA (short-dashed line), EMA-noLS (dotted line) and factorized (dash-dotted line) results. The EMA-noLS calculation coincides in all panels with the factorized (A_{TL}^{bare}) result. In the right hand panel EMA, as well as EMA-noLS, coincides with the factorized (A_{TL}^{bare}) result.

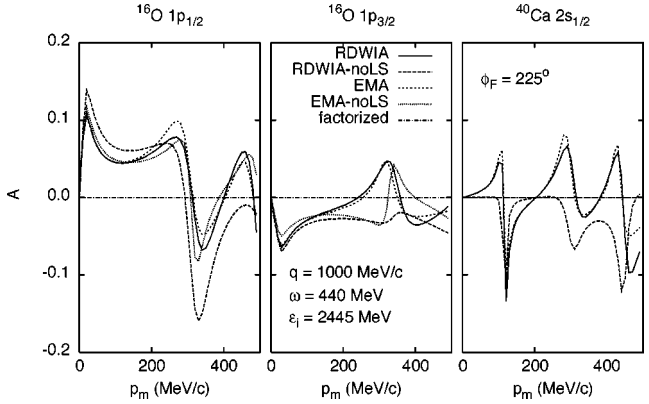

FIG. 3. Electron analyzing power A at (q,ω) constant kinematics and azimuthal angle ϕ_F=225°. The labeling of the curves is as in Fig. 2. For this observable factorization is only achieved in the EMA-noLS curve on the right hand panel. See text for details.

from factorization) are more noticeable at $|p_m|>250$ MeV/c in the $p_m<0$ region. Nonrelativistic calculations would generally yield results on the line of the EMA ones presented here. Note also that, the reduced cross section in EMA practically coincides with ρ_{DW} for the $s_{1/2}$ orbital in ^{40}Ca, and even in the ^{16}O $p_{1/2}$ and $p_{3/2}$ orbitals the reduced cross sections in EMA and ρ_{DW} are rather close in the whole p_m range.

In Figs. 2–4 we show the TL asymmetry, electron analyzing power, induced polarization and transferred polarizations, respectively, for proton knockout from the $p_{1/2}$ (left panels), $p_{3/2}$ (middle) in ^{16}O and $s_{1/2}$ (right) shells in ^{40}Ca. Results are computed for CC2 current operator and Coulomb gauge. The bound nucleon wave function corresponds to the nonlinear set of Sharma (NLSH) [24–27] and the outgoing nucleon wave function has been derived using the energy dependent A-independent relativistic optical potential fitted to ^{16}O (EDAIO) parametrization [28]. As in the previous figure, the selected kinematics corresponds to the experimental conditions of the experiments E89003 and E89033 performed at Jlab [29–31]. This is (q,ω) constant kinematics with q=1 GeV/c, ω=440 MeV and the electron beam energy fixed to ε_i=2.445 GeV. Coplanar kinematics, with ϕ_F =0°, are chosen for computing the polarization asymmetries.

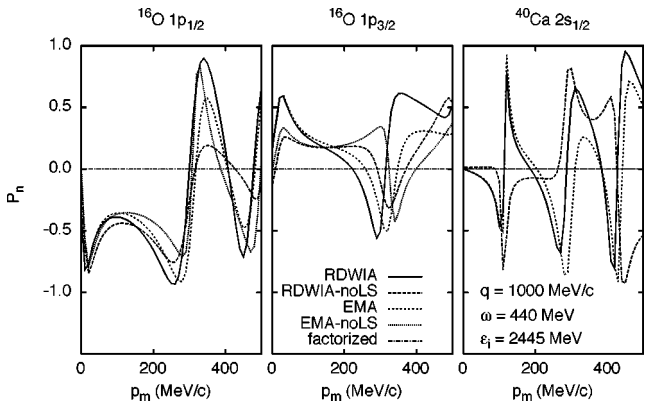

FIG. 4. Induced polarization P_n at coplanar kinematics with ϕ_F=0°. Kinematics and labeling as in Fig. 2. Only the EMA-noLS calculation for a $s_{1/2}$ shell factorizes.

TABLE I. Properties of factorization of different observables using the EMA approximation and turning off the spin-orbit coupling in the initial wave function (first column), in the final wave function (second column) or in both simultaneously (third column).

	No LS initial	No LS final	No LS both
A_{TL}	A_{TL}^{bare}	A_{TL}^{bare}	A_{TL}^{bare}
A			0
P_n			0
P_l			0
P_s			0
P'_n		$P_n'^{bare}$	$P_n'^{bare}$
P'_l		$P_l'^{bare}$	$P_l'^{bare}$
P_s		$P_s'^{bare}$	$P_s'^{bare}$

Therefore, as $P_l=P_s=P'_n=0$ when ϕ_F=0°, they are not plotted. In each graph, we show five curves corresponding to the following approaches: RDWIA (solid), RDWIA but without spin-orbit coupling in the final nucleon state, denoted as RDWIA-noLS (dashed), EMA (short-dashed), EMA-noLS (dotted), and finally the factorized result (dash-dotted).

As shown in Sec. III, factorization only holds within the EMA approach and assuming specific conditions on the spin dependence in the problem. In Table I we summarize the basic assumptions within EMA that lead to factorization for the different observables. To simplify the discussion of the results that follows we consider each observable separately.

The asymmetry A_{TL}, presented in Fig. 2, shows that factorization emerges within EMA in the case of the $s_{1/2}$ shell (where EMA, EMA-noLS and factorized results coincide). For spin-orbit dependent bound states ($p_{1/2}$ and $p_{3/2}$), factorization emerges only when there is no spin-orbit coupling in the final state (EMA-noLS coincides with factorized results). Also note that the oscillatory behavior shown by A_{TL} in RDWIA and in RDWIA-noLS is almost entirely lost within EMA, even when there is no factorization. This reflects the crucial role played by the dynamical enhancement of the lower components of the nucleon wave functions for this observable. The spin dependence in the final nucleon state modifies significantly the values of A_{TL} even at low missing momentum, but preserves its general oscillatory structure, compare for instance RDWIA vs RDWIA-noLS or EMA vs EMA-noLS.

The electron analyzing power A is presented in Fig. 3. This observable is zero in coplanar kinematics so the azimuthal angle is fixed to ϕ_F=225° in Fig. 3, but the remarks that follow also apply to other $\phi_F\neq 0°$, 180° values. As we demonstrated in Sec. III, the fifth response $R^{TL'}$ involved in A only factorizes if there is no spin-orbit contribution in the initial and final nucleon wave functions. Moreover, in such situation $R^{TL'}=0$ and hence $A=0$, as occurs for $s_{1/2}$ shell within EMA-noLS in Fig. 3. From a careful inspection of Fig. 3 we also observe that the main differences between the various approaches come from the spin-orbit term in the final state. Note that the discrepancy between RDWIA and EMA (or likewise between RDWIA-noLS and EMA-noLS) is significantly smaller than the discrepancy between RDWIA and

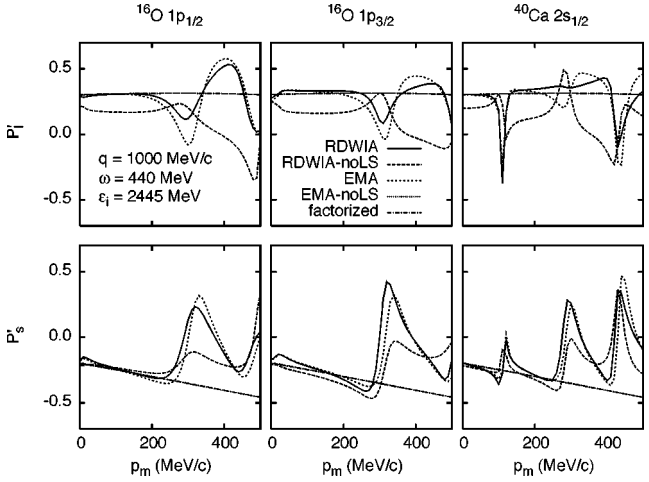

FIG. 5. Longitudinal transferred polarization P'_l (top panels) and sideways transferred polarization P'_s (bottom panels) at coplanar kinematics ($\phi_F=0°$). In this case, factorization is obtained within the EMA approach when there is no spin-orbit coupling in the final state (EMA-noLS, dotted line).

RDWIA-noLS (or EMA vs EMA-noLS). In all of the cases with $A\neq 0$, oscillations survive. The behavior of A contrasts with the one observed for the asymmetry A_{TL}. This is due to the fact that factorization is broken down already at the EMA level even in the $s_{1/2}$ shell.

The induced polarization P_n is presented in Fig. 4. Here the discussion of results follows similar trends to the previous one on A. Factorization requires no spin dependence in any of the nucleon wave functions, being the induced polarized responses equal to zero in such a case (notice that P_n is zero in the plane wave limit). In any other situation factorization breaks down and P_n shows strong oscillations in all cases. Again, it is important to point out that the behavior of the RDWIA calculation is qualitatively followed by the EMA approach, differing much more from the RDWIA-noLS or EMA-noLS. This reveals the important effects introduced by the spin-orbit coupling in the optical potential for polarized observables, contrary to what happens for the unpolarized A_{TL}.

The comment above applies also to the transferred polarizations P'_l and P'_s (Fig. 5) for which RDWIA and EMA approaches give rise to rather similar oscillating (unfactorized) results. On the contrary, RDWIA-noLS, which is also unfactorized, deviates significantly from RDWIA due to the crucial role of the spin-orbit dependence in the final state. Finally, EMA-noLS coincides with the bare asymmetries showing a flat behavior without oscillations. This is in accord with the findings in Sec. III B, where we demonstrated that the unpolarized R^α and transferred polarized $R^{\alpha'}_{l,s}$ responses factorize with the same momentum distribution function [see Table I and Eq. (34)].

VI. SUMMARY AND CONCLUSIONS

A systematic study of the property of factorization in quasielastic $(\vec{e},e'\vec{p})$ reactions has been presented. Starting from a RDWIA analysis, we have reformulated the EMA approach and studied the conditions which are needed to get factorization. In this context, we have explored the role of the spin-orbit coupling in the initial and/or final nucleon states and its influence on the breakdown of factorization.

From our general study we conclude that exact factorization only emerges within the EMA approach, i.e., neglecting the dynamical enhancement of the lower components in the nucleon wave functions by using Eq. (13). Furthermore, additional restrictions on the spin dependence in the problem are necessary to get factorization in the case of polarized observables.

Within the EMA approach, the factorization properties of various $(\vec{e},e'\vec{p})$ responses and asymmetries are as follows (see also Table I). The unpolarized R^α responses factorize to a single, polarization independent, momentum distribution when the initial or the final nucleon wave functions are independent on spin-orbit coupling (i.e., depend on ℓ but not on j). As a consequence, the A_{TL} asymmetry is in these cases given by the bare-nucleon A^{bare}_{TL} asymmetry.

The fifth response $R^{TL'}$ (and consequently A), depending on electron beam polarization, never factorizes, but becomes zero when both initial and final nucleon wave functions are independent on spin-orbit coupling, as well as in the nonrelativistic plane wave limit (PWIA).

The transferred polarization responses $R^{\alpha'}_k$ factorize when the final nucleon wave function is independent on j. Consequently the transferred polarizations are in this case given by the bare-nucleon ones, independent on whether the initial state may or may not depend on spin-orbit coupling.

The induced polarized responses R^α_k do not factorize even when the final nucleon wave function is independent on j, unless the initial wave function is also independent on j, in which case R^α_k become zero. If the final wave function depends on spin-orbit coupling but the initial wave function does not, the induced polarized responses factorize with a polarization-dependent momentum distribution different from the unpolarized one. Therefore, as stated in Eq. (32), a new factorization property emerges when there is no spin-orbit coupling in the initial state.

From our numerical calculations a clear difference in the behavior of polarized and unpolarized observables comes out. In the case of the unpolarized A_{TL} asymmetry, its general structure is not substantially modified by the final spin-orbit dependence, being much more affected by the lower components of the nucleon states. The strong oscillations in A_{TL} within RDWIA practically vanish in EMA. On the contrary, the polarized asymmetries A, P_n and $P'_{l,s}$, present a very strong sensitivity to the final spin dependence, while the general structure of the RDWIA results is preserved by the EMA calculations.

As a general conclusion, we can say that observables that require less extra assumptions (apart from EMA) to factorize, are more sensitive to any ingredient of the calculation that breaks factorization. Such observables are good candidates to test the elements of any model/calculation, as it is the case of the A_{TL} asymmetry.

In spite of the fact that factorization is not reached when realistic calculations are made, we show that the reduced

cross sections extracted from fully unfactorized calculations follow the factorized distorted momentum distribution quite well for moderate values of the missing momentum, where the bulk of the cross section lies. Then, reduced cross sections and integrated quantities directly related to them, like nuclear transparencies or inclusive cross sections, are reasonably predicted by the factorized scheme, as long as one remains at quasielastic kinematics. We may conclude that the unpolarized cross section follows closely the factorized calculation that takes FSI into account. In other words, in spite of the breakdown of factorization of the cross section introduced by FSI and by negative energy components of the relativistic model, one may still extract a meaningful effective momentum distribution within this formalism.

While the bulk of the cross section factorizes to a good approximation, ratios of cross sections like A_{TL} or polarizations are very sensitive to the ingredients of the calculation that break factorization. This is why in particular the A_{TL} observable is very sensitive to the negative energy components of the wave functions, and provides a plausible signature of the relativistic dynamics.

Contrary to A_{TL}, polarizations are much more sensitive to the spin-orbit properties of the upper components of the wave functions than to the dynamical enhancement of the lower components. Yet, RDWIA transferred polarizations closely match the factorized results in certain p_m ranges. This suggests that measuring transferred polarizations in those ranges may safely explore modifications of the nucleon form factor ratios in the nuclear medium.

ACKNOWLEDGMENTS

The authors thank T.W. Donnelly for his helpful comments. This work was partially supported by funds provided by DGI (Spain) under Contract Nos. BFM2002-03315, BFM2002-03562, FPA2002-04181-C04-04, and BFM2003-04147-C02-01 and by the Junta de Andalucía (Spain). J.R.V. and M.C.M. acknowledge financial support from the Consejería de Educación de la Comunidad de Madrid and the Fundación Cámara (University of Sevilla), respectively.

APPENDIX A: HADRONIC BARE-NUCLEON TENSOR

In this appendix we present in more detail the hadronic bare-nucleon tensor (25), which can be written using traces in the form

$$\mathcal{W}^{\mu\nu}_{ss',hh'} = \mathrm{Tr}[\bar{\hat{J}}^{\mu} u(\boldsymbol{p}_F,s)\overline{u}(\boldsymbol{p}_F,s')\hat{J}^{\nu}u(\boldsymbol{p}_I,h')\overline{u}(\boldsymbol{p}_I,h)], \tag{A1}$$

where we use the notation $\bar{\hat{J}}^{\mu} \equiv \gamma^0 \hat{J}^{\mu\dagger}\gamma^0$.

Making use of the following relation [17,18]:

$$u(\boldsymbol{p},s)\overline{u}(\boldsymbol{p},s') = \frac{\delta_{ss'} + \gamma_5 \not{\varphi}_{ss'}}{2}\frac{\not{P}+M}{2M}, \tag{A2}$$

with $\varphi^{\mu}_{ss'}$, a pseudovector defined as $\varphi^{\mu}_{ss'} = \overline{u}(\boldsymbol{p},s')\gamma^{\mu}\gamma^5 u(\boldsymbol{p},s)$ which reduces to the four spin S^{μ} in the diagonal case, i.e., $\varphi^{\mu}_{ss}=S^{\mu}$, the bare nucleon tensor reads

$$\begin{aligned}\mathcal{W}^{\mu\nu}_{ss',hh'} = {} & \frac{1}{16M^2}\mathrm{Tr}[\bar{\hat{J}}^{\mu}(\not{P}_F+M)\hat{J}^{\nu}(\not{P}_I+M)]\delta_{ss'}\delta_{hh'} \\ & + \frac{1}{16M^2}\mathrm{Tr}[\bar{\hat{J}}^{\mu}(\not{P}_F+M)\hat{J}^{\nu}\gamma_5\not{\varphi}_{hh'}(\not{P}_I+M)]\delta_{ss'} \\ & + \frac{1}{16M^2}\mathrm{Tr}[\bar{\hat{J}}^{\mu}\gamma_5\not{\varphi}_{ss'}(\not{P}_F+M)\hat{J}^{\nu}(\not{P}_I+M)]\delta_{hh'} \\ & + \frac{1}{16M^2}\mathrm{Tr}[\bar{\hat{J}}^{\mu}\gamma_5\not{\varphi}_{ss'}(\not{P}_F+M)\hat{J}^{\nu}\gamma_5\not{\varphi}_{hh'}(\not{P}_I+M)].\end{aligned} \tag{A3}$$

This result is expressed in a compact form in Eq. (27).

APPENDIX B: NO SPIN-ORBIT IN THE EJECTED NUCLEON WAVE FUNCTION

Let us consider the case of no spin-orbit coupling in the final nucleon wave function. This means that the radial functions g_{κ} and δ_{κ} depend only on l but not on j. Then the upper component of the wave function is given by

$$\begin{aligned}\psi^{s_F}_{F,up}(\boldsymbol{p}) &= 4\pi\sqrt{\frac{E_F+M}{2E_F}}\sum_{\ell m} e^{-i\delta^*_{\ell}}Y^{m*}_{\ell}(\hat{\boldsymbol{p}}_F)g^*_l(p) \\ &\times\sum_{j\mu}\left\langle \ell m\frac{1}{2}s_F|j\mu\right\rangle\Phi^{\mu}_{\kappa}(\hat{\boldsymbol{p}}) \\ &= G(\boldsymbol{p},\boldsymbol{p}_F)\chi_{s_F}\end{aligned} \tag{B1}$$

with

$$G(\boldsymbol{p},\boldsymbol{p}_F) = 4\pi\sqrt{\frac{E_F+M}{2E_F}}\sum_{\ell m} e^{-i\delta^*_{\ell}}Y^{m*}_{\ell}(\hat{\boldsymbol{p}}_F)g^*_l(p)Y^{m}_{\ell}(\hat{\boldsymbol{p}}). \tag{B2}$$

The resulting wave function for the ejected proton is then

$$\psi^{s_F\ EMA}_{F}(\boldsymbol{p}) = \sqrt{\frac{2M}{E_F+M}}G(\boldsymbol{p},\boldsymbol{p}_F)u(\boldsymbol{p}_F,s_F). \tag{B3}$$

Introducing this result into the expression of the current matrix element, we get

$$J^{\mu}_{EMA} = \sum_{m_{\ell_b}h}\left\langle \ell_b m_{\ell_b}\frac{1}{2}h|j_b\mu_b\right\rangle[\overline{u}(\boldsymbol{p}_F,s_F)\hat{J}^{\mu}u(\boldsymbol{p}_I,h)]U^{m_{\ell_b}}_{\kappa_b}(\boldsymbol{p}_F,\boldsymbol{q}) \tag{B4}$$

being,

$$\begin{aligned}U^{m_{\ell_b}}_{\kappa_b}(\boldsymbol{p}_F,\boldsymbol{q}) &= \frac{2M}{\sqrt{(E_I+M)(E_F+M)}}(-i)^{\ell_b} \\ &\times\int dp G^*(\boldsymbol{p}+\boldsymbol{q},\boldsymbol{p}_F)g_{\kappa_b}(p)Y^{m_{\ell_b}}_{\ell_b}(\hat{\boldsymbol{p}}).\end{aligned} \tag{B5}$$

We observe that the whole dependence on the spin polarization s_F is contained in the Dirac spinor $u(\boldsymbol{p}_F,s_F)$. From

Eq. (B4) we can immediately construct the hadronic tensor $W^{\mu\nu}_{EMA}$, which can be written in the form of Eq. (33) with the momentum distribution function given by

$$\widetilde{N}_{hh'}(\boldsymbol{p}_F,\boldsymbol{q}) = \frac{1}{2j_b+1}\sum_{\mu_b}\sum_{m_{\ell_b}m_{\ell_b}}\left\langle \ell_b m_{\ell_b}\frac{1}{2}h|j_b\mu_b\right\rangle \times\left\langle \ell_b m'_{\ell_b}\frac{1}{2}h'|j_b\mu_b\right\rangle U^{m_{\ell_b}*}_{\kappa_b}U^{m'_{\ell_b}}_{\kappa_b}. \quad \text{(B6)}$$

As a particular example, let us consider the case of the plane wave limit without dynamical relativistic effects. In this situation the function $G(\boldsymbol{p},\boldsymbol{p}_F)$ [Eq. (B5)] simply reduces to

$$G^{PW}(\boldsymbol{p},\boldsymbol{p}_F) = \sqrt{\frac{E_F+M}{2E_F}}(2\pi)^{3/2}\delta^3(\boldsymbol{p}-\boldsymbol{p}_F), \quad \text{(B7)}$$

and the momentum distribution results

$$\widetilde{N}^{PW}_{hh'}(\boldsymbol{p}_F,\boldsymbol{q}) = \delta_{hh'}\frac{M^2}{2E_IE_F}(2\pi)^3N^{EMA}(p_I). \quad \text{(B8)}$$

[1] S. Boffi, C. Giusti, F. D. Pacati, and M. Radici, Phys. Rep. **226**, 1 (1993); *Electromagnetic Response of Atomic Nuclei* (Oxford University Press, Oxford, 1996).
[2] J. J. Kelly, Adv. Nucl. Phys. **23**, 75 (1996).
[3] S. Frullani and J. Mougey, Adv. Nucl. Phys. **14**, 1 (1985).
[4] A. Picklesimer and J. W. Van Orden, Phys. Rev. C **35**, 266 (1987).
[5] A. Picklesimer and J. W. Van Orden, Phys. Rev. C **40**, 290 (1989).
[6] J. M Udías, P. Sarriguren, E. Moya de Guerra, E. Garrido, and J. A. Caballero, Phys. Rev. C **48**, 2731 (1993).
[7] J. M Udías, P. Sarriguren, E. Moya de Guerra, E. Garrido, and J. A. Caballero, Phys. Rev. C **51**, 3246 (1995).
[8] J. M. Udías, P. Sarriguren, E. Moya de Guerra, and J. A. Caballero, Phys. Rev. C **53**, R1488 (1996).
[9] J. M. Udías, J. A. Caballero, E. Moya de Guerra, J. E. Amaro, and T. W. Donnelly, Phys. Rev. Lett. **83**, 5451 (1999).
[10] J. M. Udías and J. R. Vignote, Phys. Rev. C **62**, 034302 (2000).
[11] J. M. Udías, J. A. Caballero, E. Moya de Guerra, J. R. Vignote, and A. Escuderos, Phys. Rev. C **64**, 024614 (2001).
[12] F. Kazemi Tabatabei, J. E. Amaro, and J. A. Caballero, Phys. Rev. C **68**, 034611 (2003).
[13] A. Meucci, C. Giusti, and F. D. Pacati, Phys. Rev. C **64**, 014604 (2001); nucl-th/0211023.
[14] A. Meucci, Phys. Rev. C **65**, 044601 (2002).
[15] J. Ryckebusch, D. Debruyne, W. Van Nespen, and S. Janssen, Phys. Rev. C **60**, 034604 (1999).
[16] M. C. Martínez, J. R. Vignote, J. A. Caballero, T. W. Donnelly, E. Moya de Guerra, and J. M. Udías, Phys. Rev. C **69**, 034604 (2004).
[17] J. A. Caballero, T. W. Donnelly, and G. I. Poulis, Nucl. Phys. **A555**, 709 (1993).
[18] J. A. Caballero, T. W. Donnelly, E. Moya de Guerra, and J. M. Udías, Nucl. Phys. **A632**, 323 (1998); **A643**, 189 (1998).
[19] S. Dieterich *et al.*, Phys. Lett. B **500**, 47 (2001).
[20] S. Strauch *et al.*, Phys. Rev. Lett. **91**, 052301 (2003).
[21] M. C. Martínez, J. A. Caballero, and T. W. Donnelly, Nucl. Phys. **A707**, 83 (2002); **A707**, 121 (2002).
[22] J. J. Kelly, Phys. Rev. C **56**, 2672 (1997); **59**, 3256 (1999).
[23] T. de Forest, Nucl. Phys. **A392**, 232 (1983).
[24] B. D. Serot, Phys. Lett. **86B**, 146 (1979).
[25] C. J. Horowitz and B. D. Serot, Nucl. Phys. **A368**, 503 (1981).
[26] C. J. Horowitz, D. P. Murdock, and B. D. Serot, *Computational Nuclear Physics* (Springer, Berlin, 1991).
[27] M. M. Sharma, M. A. Nagarajan, and P. Ring, Phys. Lett. B **312**, 377 (1993).
[28] E. D. Cooper, S. Hama, B. C. Clark, and R. L. Mercer, Phys. Rev. C **47**, 297 (1993).
[29] JLab Experiment E89-003, Spokespersons, W. Bertozzi, K. Fissum, A. Saha, and L. Weinstein (unpublished).
[30] JLab Experiment E89-033, Spokespersons, C. C. Chang, C. Glashausser, S. Nanda, and P. Rutt (unpublished).
[31] J. Gao *et al.*, Phys. Rev. Lett. **84**, 3265 (2000).